

LPCAT1 promotes melanoma cell proliferation via Akt signaling

YUQIAN WANG^{1*}, YINGJIAN HUANG^{1,2*}, YAN WANG³, WEN ZHANG¹, NING WANG¹,
RUIMIN BAI¹, RUITING LUO¹, HUIHUI TUO¹ and YAN ZHENG¹

¹Department of Dermatology, The First Affiliated Hospital of Xi'an Jiaotong University, Xi'an, Shaanxi 710061;

²Department of Dermatology, Qilu Hospital, Cheeloo College of Medicine, Shandong University, Jinan, Shandong 250012;

³Center for Mitochondrial Biology and Medicine, The Key Laboratory of Biomedical Information Engineering of Ministry of Education, Xi'an Jiaotong University School of Life Science and Technology, Xi'an, Shaanxi 710004, P.R. China

Received October 20, 2023; Accepted February 7, 2024

DOI: 10.3892/or.2024.8726

Abstract. Melanoma is the most lethal type of skin cancer with an increasing cutaneous cancer-related mortality rate worldwide. Despite therapeutic advances in targeted therapy and immunotherapy, the overall survival of patients with melanoma remains unsatisfactory. Thus, a further understanding of the pathogenesis of melanoma may aid towards the development of therapeutic strategies. Lysophosphatidylcholine acyltransferase 1 (LPCAT1) is a key enzyme that converts lysophosphatidylcholine into phosphatidylcholine in lipid remodeling. In the present study, LPCAT1 was found to play a pro-proliferative role in melanoma. Firstly, the expression of LPCAT1 was found to be upregulated in tissues from patients with melanoma compared with that in benign nevi. Subsequently, LPCAT1 knockdown was performed, utilizing short hairpin RNA, which induced melanoma cell cycle arrest at the G1/S transition and promoted cell death. Moreover, LPCAT1 facilitated melanoma cell growth in an Akt-dependent manner. In summary, the results of the present study indicate that targeting LPCAT1 may impede cell proliferation by inhibiting Akt signaling, thus providing a promising therapeutic strategy for melanoma in clinical practice.

Introduction

Melanoma is the major life-threatening form of skin cancer, accounting for 80% of cutaneous cancer-related mortality (1).

Melanoma arises from the malignant transformation of melanocytes, which produce a light-protective pigment known as melanin (2). Multiple exogenous and endogenous factors are involved in the malignant transformation of melanocytes into melanoma (3). Accessible or early-stage melanoma can be cured by surgical resection (3). However, only a limited number of clinical options were available for advanced-stage or metastatic melanoma 20 years ago. Over the past decade, the treatment of advanced-stage or metastatic melanoma has met an unprecedented series of clinical advances with an influx of novel therapeutics, including immunotherapy, targeted therapy, and their combined application (4,5). Despite the fact that these emerging therapies have improved the overall survival rate of patients, issues concerning therapeutic toxicity and acquired resistance remain unresolved (6,7). The therapeutic strategies of melanoma are based upon novel mechanistic discoveries. Therefore, it is of great benefit to further investigate the molecular mechanisms involved in the development of melanoma and exploit therapeutic targets for its treatment.

Lysophosphatidylcholine acyltransferase 1 (LPCAT1) was first reported in 2006 by two groups, independently (8,9). LPCAT1 is integral for phospholipid remodeling. There are two strategies which can be used to generate phosphatidylcholine: i) *De novo* synthesis known as the Kennedy pathway (10); and ii) phospholipid remodeling known as the Lands cycle (11). In comparison to *de novo* synthesis, phospholipid remodeling accounts for a substantial part of the diverse and asymmetrical distribution of fatty acyl chains in phospholipids. LPCAT1 is a crucial enzyme, involved in the remodeling pathway by converting lysophosphatidylcholine to phosphatidylcholine. Due to the physiological function, LPCAT1 is fundamental for pulmonary surfactant homeostasis (12), lipid droplet formation (13), non-inflammatory platelet-activating factor remodeling (14) and retinal photoreceptor homeostasis (15,16). LPCAT1 regulates lipid metabolism in tumor cells and its expression is upregulated in various types of cancer, including cutaneous squamous cell carcinoma (17), lung adenocarcinoma (18), glioblastoma (19), hepatocellular carcinoma (20,21), clear cell renal cell carcinoma (22), oral squamous cell carcinoma (23), prostate cancer (24,25), colorectal cancer (26), breast cancer (27), endometrial cancer (28) and esophageal cancer (29).

Correspondence to: Professor Yan Zheng, Department of Dermatology, The First Affiliated Hospital of Xi'an Jiaotong University, 277 West Yanta Road, Xi'an, Shaanxi 710061, P.R. China
E-mail: zenyang66@126.com

*Contributed equally

Abbreviations: LPCAT1, lysophosphatidylcholine acyltransferase 1; Akt, protein kinase B; shRNA, short hairpin RNA

Key words: LPCAT1, melanoma, proliferation, apoptosis, Akt signaling

In the present study, the expression of LPCAT1 in melanoma and benign nevi from patients were examined. Short hairpin (sh)RNA was utilized to stably knock down LPCAT1 in melanoma cell lines. Melanoma cell viability was measured following LPCAT1 knockdown. Cell cycle analysis and cell apoptosis analysis were carried out to investigate LPCAT1-regulated cell proliferation. Additionally, the expression levels of cell cycle and cell apoptosis regulators were measured following LPCAT1 knockdown. Ultimately, the underlying mechanisms of LPCAT1-regulated melanoma cell proliferation were further investigated.

Materials and methods

Patient samples. A total number of 68 paraffin-embedded section samples from patients with melanoma (23 males and 17 females; age range, 36-84 years) and patients with nevi (16 males and 12 females; age range, 20-55 years) were collected from the Department of Dermatology at the First Affiliated Hospital of Xi'an Jiaotong University (Xi'an, China). The study was approved by the Ethics Committee of the First Affiliated Hospital of Xi'an Jiaotong University (approval no. LLSBPJ-2023-222). Written informed consent was obtained from the patients prior to sample collection.

Immunohistochemistry. Paraffin-embedded (4% paraformaldehyde for 24 h at 37°C) melanoma tissues and benign nevi were sectioned into 4- μ m-thick slices, deparaffinized and rehydrated with graded ethanol dilutions. Following antigen retrieval in Tris/EDTA (pH 9.0) buffer and endogenous peroxidase activity blockade in 3% hydrogen peroxide (ANNJET, Inc.; <http://www.ajxd.com/product/24/>), the sections were blocked using 3% BSA (Wuhan Servicebio Technology Co., Ltd.) for 30 min at room temperature. The sections were then incubated with anti-LPCAT1 antibody (1:200; cat. no. ab214034; Abcam) overnight at 4°C. After washing and drying, the tissues were covered with HRP-labeled anti-rabbit secondary antibody (1:200; cat. no. GB23303; Wuhan Servicebio Technology Co., Ltd.) at room temperature for 50 min. Detection was achieved by DAB (cat. no. G1212; Wuhan Servicebio Technology Co., Ltd.) chromogenic reaction for 15 min and hematoxylin counterstaining (cat. no. G1004; Wuhan Servicebio Technology Co., Ltd.) for 3 min at room temperature. Subsequently, routine dehydration and mounting were performed. The staining images were analyzed under a microscope (E100, Nikon Instruments Co., Ltd.) by two pathologists independently. The staining intensity was scored as follows: i) 0, none; ii) 1, weak intensity; iii) 2, moderate intensity; and iv) 3, strong intensity. The percentages of positive cells were scored as follows: i) 0, 0-5%; ii) 1, 6-25%; iii) 2, 26-50%; iv) 3, 51-75%; and v) 4, 76-100%. The staining score of each field was the product of the staining intensity and percentage. The final score for each section was calculated as the average of five fields.

Immunofluorescence staining. Paraffin-embedded (4% paraformaldehyde for 24 h at 37°C) melanoma tissues and benign nevi were sectioned, deparaffinized and rehydrated. Following antigen repair, the tissue sections were blocked using 3% BSA for 30 min at room temperature. Subsequently, the sections were incubated with anti-MelanA antibody

(1:1,000; cat. no. ab210546; Abcam) overnight at 4°C, followed by HRP-labeled anti-rabbit secondary antibody (1:500; cat. no. GB23303; Wuhan Servicebio Technology Co., Ltd.) for 50 min at room temperature. Subsequently, the sections were incubated with tyramide signal amplification-fluorescein isothiocyanate (TSA-FITC; cat. no. G1222; Wuhan Servicebio Technology Co., Ltd.) for 10 min at room temperature. After washing with TBST (Wuhan Servicebio Technology Co., Ltd.) three times (for 5 min each), the sections were immersed in EDTA antigen retrieval buffer (pH 8.0) (Wuhan Servicebio Technology Co., Ltd.) and maintained at 95-100°C for 15 min to remove the antibodies combined with tissue. Subsequently, the sections were incubated with anti-LPCAT1 antibody (1:200; cat. no. ab214034; Abcam) overnight at 4°C, followed by Alexa Fluor anti-rabbit 555 antibody (cat. no. A0453; Beyotime Institute of Biotechnology) for 50 min at room temperature. Nuclei were stained with DAPI (cat. no. D1306; Thermo Fisher Scientific, Inc.) for 10 min at room temperature. Images were collected using a digital slide scanner (Pannoramic 250 FLASH; 3DHISTECH, Ltd.).

Cell lines and cell culture. Human melanoma cell lines A375 (cat. no. CL-0014) and A2058 (cat. no. CL-0652) were purchased from Procell Life Science & Technology Co., Ltd. in 2021. Both cell lines were authenticated using short tandem repeat fingerprinting and tested for mycoplasma contamination (data not shown). The cells were cultured in DMEM (cat. no. 11995065; Gibco; Thermo Fisher Scientific, Inc.) with 10% fetal bovine serum (cat. no. 04-001-1Acs; Biological Industries; Sartorius AG) and 1% penicillin-streptomycin-glutamine (cat. no. 10378016; Gibco; Thermo Fisher Scientific, Inc.). The cells were incubated at 37°C in a humidified incubator with 5% CO₂. The 293T cell line (cat. no. GNHu17) was purchased from the National Collection of Authenticated Cell Cultures and used for lentivirus packaging.

Lentivirus-mediated gene knockdown and overexpression. LPCAT1 knockdown, overexpression and corresponding control lentivirus were all synthesized by Shanghai GenePharma Co., Ltd. The sequences of LPCAT1 lentiviral vector-based shRNAs and corresponding control have been described in a previous study by the authors (17). Briefly, lentivirus particles were prepared by transfecting 293T cells in 15-cm dishes with 0.5 μ g either gene-specific shRNA plasmids or shuttle plasmids containing target sequences along with lentiviral packaging plasmids (pGag/Pol, pRev, pVSV-G) in a 4:3:1 ratio for 72 h at 37°C (3rd generation system was used). Virus-containing media was then collected and used to infect A375 and A2058 cells to establish stable LPCAT1-knockdown and overexpression cell lines in the presence of 5 μ g/ml polybrene (MOI=10 in both cell lines). Following 48 h of infection, stable clones were selected using puromycin (5 μ g/ml; cat. no. ST551; Beyotime Institute of Biotechnology) for 14 consecutive days. The LPCAT1 knockdown and overexpression efficiencies were verified using reverse transcription-quantitative PCR (RT-qPCR) and western blot analysis.

RT-qPCR. Total RNA was extracted from the cells using TRIzol[®] reagent (15596026; Invitrogen; Thermo Fisher Scientific, Inc.). cDNA was synthesized using PrimeScript Master Mix (cat.

no. RR036A; Takara Bio, Inc.) incubated in 37°C for 60 min and 85°C for 15 sec. qPCR was performed using TB Green® Premix Ex Taq™ II (cat. no. RR820B; Takara Bio, Inc.). The cycling conditions applied were as follows: 95°C for 10 min; 35 cycles including 95°C for 30 sec, 55°C for 30 sec and 72°C for 20 sec; 72°C for 10 min. The mRNA level of LPCAT1 was analyzed using the 2^{-ΔΔC_q} method (30). GAPDH was chosen as an internal control. The primers used in the present study were the same as those in a previously published study by the authors (17).

Western blot analysis. Total protein was extracted from the cells using cell lysis buffer (cat. no. P0013; Beyotime Institute of Biotechnology) containing phenylmethylsulfonyl fluoride. The quantification of protein concentration was carried out using the Pierce BCA Protein Assay Kit (cat. no. 23227; Thermo Fisher Scientific, Inc.). Proteins (20 μg) were separated using SDS-PAGE on 10 or 12% tris-glycine gels and transferred onto PVDF membrane (cat. no. ISEQ00010; MilliporeSigma). The PVDF membrane was blocked using 5% fat-free milk for 1 h at room temperature. Subsequently, the membrane was incubated with primary antibodies overnight at 4°C, followed by a horseradish peroxidase (HRP)-conjugated secondary antibody for 1 h at room temperature. Protein bands were visualized using Clarity Western ECL Substrate (cat. no. 1705060; Bio-Rad Laboratories, Inc.). The primary antibodies used were as follows: Anti-LPCAT1 (1:1,000; cat. no. ab214034; Abcam), anti-cyclin A (1:1,000; cat. no. sc-596; Santa Cruz Biotechnology, Inc.), anti-cyclin B1 (1:1,000; cat. no. sc-595; Santa Cruz Biotechnology, Inc.), anti-cyclin D1 (1:1,000; sc-246; Santa Cruz Biotechnology, Inc.), anti-cyclin E (1:1,000; cat. no. sc-377100; Santa Cruz Biotechnology, Inc.), anti-caspase-3 (1:1,000; cat. no. 14220; Cell Signaling Technology, Inc.), anti-Bcl-2 (1:1,000; cat. no. 3498; Cell Signaling Technology, Inc.), anti-Bcl-xL (1:1,000; cat. no. 2764; Cell Signaling Technology, Inc.), anti-BCL2 antagonist/killer 1 (BAK; 1:1,000; cat. no. 12105; Cell Signaling Technology, Inc.), anti-Akt (1:1,000; cat. no. 9272; Cell Signaling Technology, Inc.), anti-phosphorylated (p-)Akt (Ser473; 1:1,000; cat. no. 9271; Cell Signaling Technology, Inc.) and anti-β-actin (1:3,000; cat. no. 3700; Cell Signaling Technology, Inc.). The secondary antibodies used were anti-rabbit IgG (1:3,000; cat. no. 7074; Cell Signaling Technology, Inc.) and anti-mouse IgG (1:3,000; cat. no. 7076; Cell Signaling Technology, Inc.).

Cell viability analysis. Cell viability was measured using a Cell Counting Kit-8 (CCK-8; cat. no. CK04; Dojindo Laboratories, Inc.). Melanoma cells were seeded in 96-well plates, at a density of 5,000 cells/well and cultured overnight in the incubator at 37°C. Cell viability was assessed after 0, 24, 48 and 72 h, respectively. At each indicated time point, the cells were incubated with 10 μl/well CCK-8 reagent for an additional 2 h at 37°C. Finally, the optical density value was measured at 450 nm by a microplate reader (Thermo Fisher Scientific, Inc.). For the cell viability with Akt inhibitor, LPCAT1 overexpression and control cells were seeded in 96-well plates overnight. Cell viability was measured at 0 h. Subsequently, LPCAT1-overexpressing and control cells were treated with 10 μM Akt inhibitor (MK-2206; cat. no. S1078; Selleck Chemicals) or DMSO for 24, 48 or 72 h, and cell viability was measured. All assays were repeated three times.

Cell cycle analysis. Melanoma cells transfected with LPCAT1 shRNA and control shRNA were synchronized by serum starvation for 48 h, followed by incubation in 37°C serum (cat. no. 04-001-1Acs; Biological Industries; Sartorius AG) for a further 48 h. The cells were then harvested using trypsin (cat. no. C0201; Beyotime Institute of Biotechnology) and fixed in 70% cold ethanol at -20°C overnight. After washing with cold PBS, the fixed cells were collected by centrifugation (4°C, 107 x g, 5 min) and suspended in propidium iodide (PI)/RNase Staining Buffer (cat. no. CA1510; Beijing Solarbio Science & Technology Co., Ltd.) for 30 min in the dark at 37°C. The cell cycle was analyzed using flow cytometry (NovoCyte; Agilent Technologies, Inc.). Assays were repeated three times. NovoExpress was used for subsequent analysis.

Cell apoptosis analysis. The melanoma cells transfected with LPCAT1 shRNA and control shRNA were harvested using trypsin (cat. no. C0201; Beyotime Institute of Biotechnology), washed twice using cold PBS (Wuhan Servicebio Technology Co., Ltd.) and suspended in binding buffer (from Annexin V-FITC/PI apoptosis detection kit below-mentioned). The cells were stained with Annexin V-FITC and PI (cat. no. 556547; BD Biosciences). Cell apoptosis was analyzed using flow cytometry (NovoCyte; Agilent Technologies, Inc.). The assays were repeated three times.

Statistical analysis. Data are presented as the mean ± SEM from three independent experiments. Statistical analyses were performed with GraphPad Prism 8.0 (Dotmatics). An unpaired Student's t-test was used for comparing two groups, and one-way ANOVA with Bonferroni's post hoc multiple comparison test was used for comparing multiple groups. P<0.05 was considered to indicate a statistically significant difference.

Results

LPCAT1 expression is highly upregulated in melanoma. To explore the role of LPCAT1 in melanoma, the expression levels of LPCAT1 in tissues from patients with melanoma and benign nevi were first examined. The results of immunohistochemical staining revealed that the expression of LPCAT1 was higher in the melanoma tissues in comparison with that in benign nevi (Fig. 1A). The staining score of LPCAT1 expression was significantly higher in human melanoma tissues in comparison with benign nevi (Fig. 1A), which was in line with the results from subsequent immunofluorescence analysis (Fig. 1B). Meanwhile, LPCAT1 was mainly localized in the cytoplasm (Fig. 1B). Overall, these results demonstrated that LPCAT1 expression is upregulated in melanoma.

LPCAT1 knockdown impairs melanoma cell viability. The effects of LPCAT1 on melanoma cell viability were then investigated. Lentivirus transfection was employed to establish stable LPCAT1 knockdown A375 and A2058 cell lines. To rule out the potential off-target effect, two independent LPCAT1 specific shRNAs were transfected, respectively. The knockdown efficiencies were measured. As demonstrated in Fig. 2A and B, the mRNA and protein levels of LPCAT1 were significantly downregulated in the shLPCAT1 groups

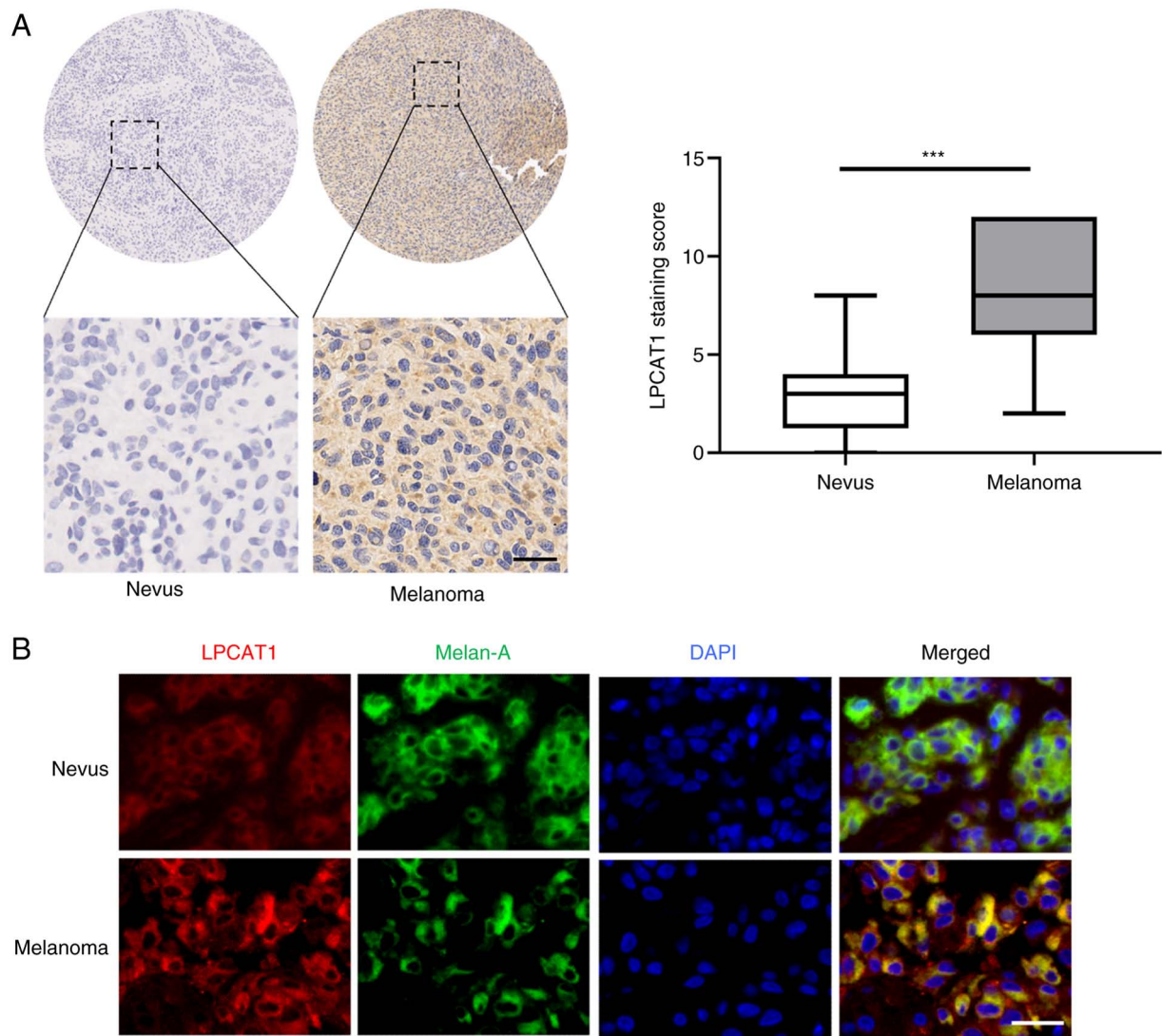


Figure 1. Upregulation of LPCAT1 expression in melanoma. (A) Immunohistochemical staining of LPCAT1 in benign nevi and melanoma tissues. The images on the bottom are enlarged images of the boxed area on the top. Magnification, $\times 5$; scale bar, $50 \mu\text{m}$. (B) Immunofluorescence staining of LPCAT1 in benign nevi and melanoma tissues. Scale bar, $50 \mu\text{m}$. *** $P < 0.001$. LPCAT1, lysophosphatidylcholine acyltransferase 1.

compared with control groups in the A375 and A2058 cell lines. Cell viability detection demonstrated that the genetic depletion of LPCAT1 resulted in the attenuation of cell viability (Fig. 2C). As a result, LPCAT1 knockdown impaired the proliferative ability of the melanoma cells.

LPCAT1 knockdown induces G1/S arrest in the melanoma cell cycle. Cell cycle analyses were performed to examine the effects of LPCAT1 on melanoma cell proliferation. Flow cytometric analysis revealed delayed cell cycle progression in the G1/S transition following LPCAT1 knockdown in the A375 and A2058 cells, with the percentage of cells being increased in the G1 phase and decreased in the S phase (Fig. 3A and B). The expression of cell cycle regulators was then detected. The expression of cyclin D1 was downregulated following LPCAT1 knockdown, whereas the protein levels of cyclin A, cyclin B1 and cyclin E were not markedly affected in both cell lines (Fig. 3C). Therefore, LPCAT1 knockdown induced G1/S arrest by decreasing cyclin D1 expression in melanoma cells.

LPCAT1 knockdown promotes melanoma cell apoptosis. It was demonstrated that LPCAT1 knockdown attenuated melanoma cell proliferation by altering the cell cycle. Subsequently, the present study investigated whether cell apoptosis was involved in the LPCAT1-regulated melanoma cell proliferation. As presented in Fig. 4A and B, LPCAT1 knockdown induced the extensive apoptosis of melanoma cells, with increases of 10 to 20% in the apoptotic rates in the shLPCAT1 groups, as compared with the control groups. The increased apoptotic rate was associated with the upregulated expression levels of cleaved caspase-3 and BAK, as well as the downregulated expression levels of Bcl-2 and Bcl-xL following LPCAT1 knockdown in the A375 and A2058 cells (Fig. 4C). Overall, LPCAT1 knockdown promoted melanoma cell apoptosis by increasing cleaved caspase-3 and BAK expression, and decreasing Bcl-2 and Bcl-xL expression.

LPCAT1 facilitates melanoma cell growth via the Akt signaling pathway. The present study then investigated the mechanism underlying LPCAT1-regulated cell proliferation

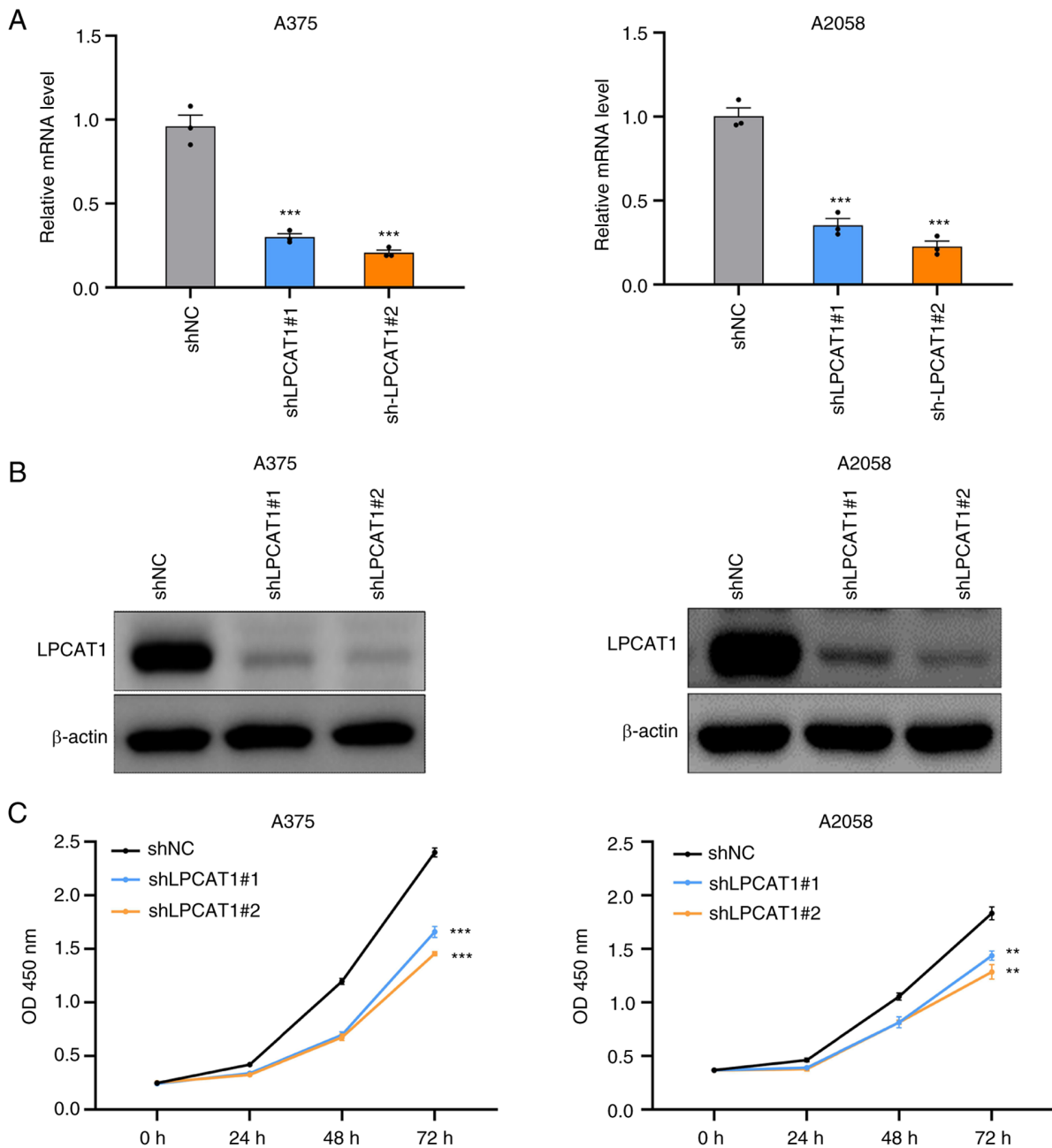


Figure 2. LPCAT1 knockdown impairs melanoma cell growth. (A) Relative mRNA level of LPCAT1 in A375 and A2058 cells expressing control and LPCAT1 shRNA. (B) Western blot analysis of LPCAT1 in A375 and A2058 cells transfected with control and LPCAT1 shRNA. (C) Viability of A375 and A2058 cells transfected with control and LPCAT1 shRNA. Data represent the mean \pm SEM of triplicates. ** $P < 0.01$ and *** $P < 0.001$ vs. shNC. LPCAT1, lysophosphatidylcholine acyltransferase 1; OD, optical density; shNC, short hairpin RNA targeting negative control; shLPCAT1, short hairpin RNA targeting LPCAT1.

in melanoma. Numerous studies have revealed that Akt plays a critical role in melanoma cell proliferation (1-3). The protein levels of Akt and p-Akt after LPCAT1 knockdown were thus analyzed. The phosphorylation of Akt at Ser773 was decreased in the shLPCAT1 group (Fig. 5A). Subsequently, LPCAT1 overexpression was induced in A375 and A2058 cell lines using LPCAT1 overexpression lentivirus. LPCAT1 overexpression efficiency was analyzed (Fig. 5B and C). Moreover, the expression levels of p-Akt at Ser773 were upregulated in the LPCAT1-overexpressing cells (Fig. 5C). LPCAT1 overexpression promoted melanoma cell proliferation (Fig. 5D). To determine whether the Akt pathway mediates LPCAT1-regulated melanoma cell proliferation,

LPCAT1-overexpressing cells and control cells were treated with the Akt specific inhibitor, MK-2206. Treatment with MK-2206 resulted in the suppression of the proliferation of the melanoma cells (Fig. 5D). Moreover, MK-2206 reversed the enhanced proliferation induced by LPCAT1 (Fig. 5D). Overall, LPCAT1 promoted melanoma cell proliferation in an Akt-dependent manner.

Discussion

Melanoma is a tumor entity presenting with significant metabolic plasticity. The malignant transformation from melanocyte to melanoma is markedly influenced by oncogenic signaling and

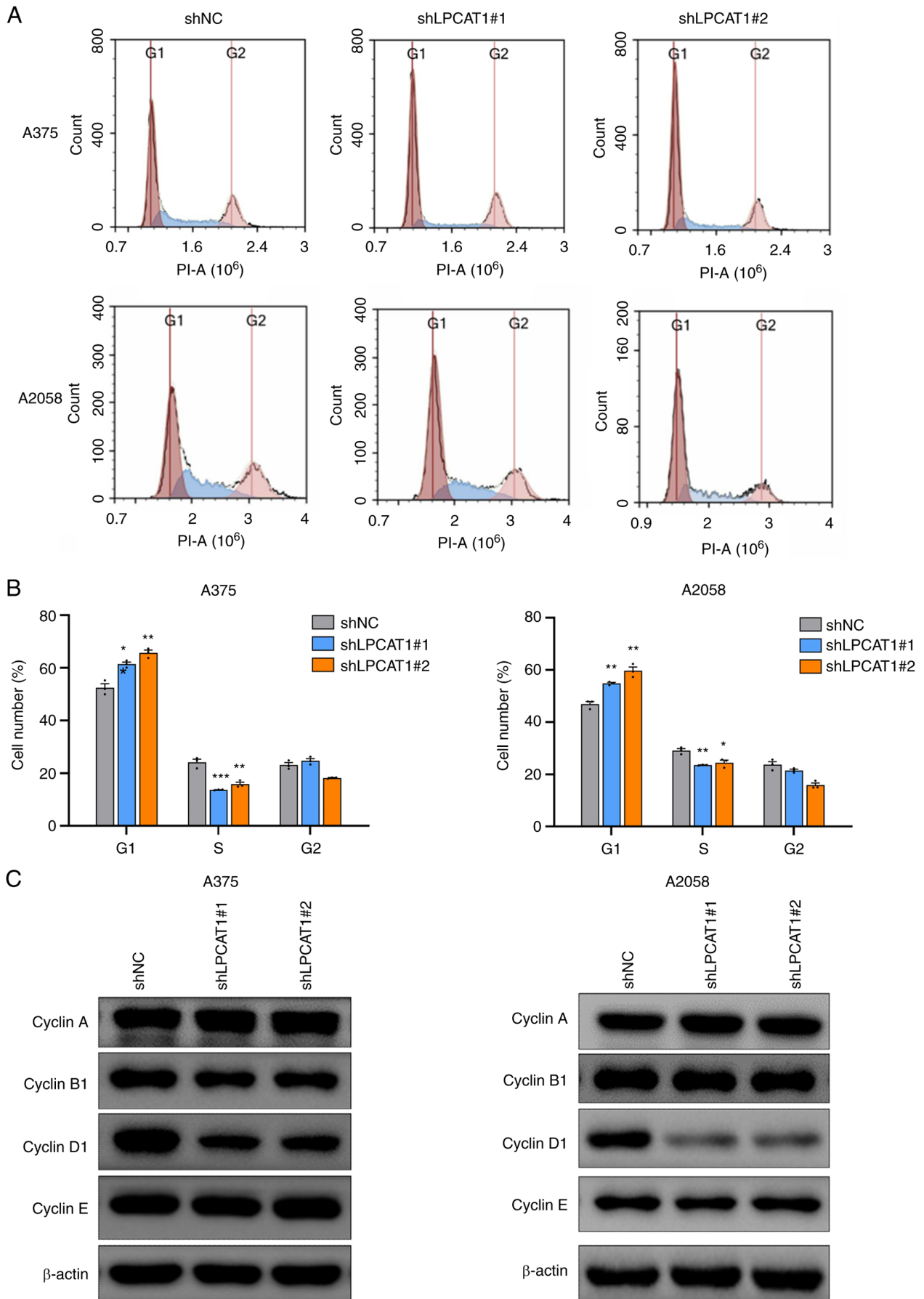


Figure 3. LPCAT1 knockdown induces G1/S arrest in the melanoma cell cycle. (A) Flow cytometric analysis of the cell cycle of A375 and A2058 cells transfected with control and LPCAT1 shRNA. (B) Quantification of the cell cycle in (A). (C) Western blot analysis of cell cycle regulators in A375 and A2058 cells transfected with control and LPCAT1 shRNA. Data represent the mean \pm SEM of triplicates. * $P < 0.05$, ** $P < 0.01$ and *** $P < 0.001$, vs. shNC. LPCAT1, lysophosphatidylcholine acyltransferase 1; shNC, short hairpin RNA targeting negative control; shLPCAT1, short hairpin RNA targeting LPCAT1.

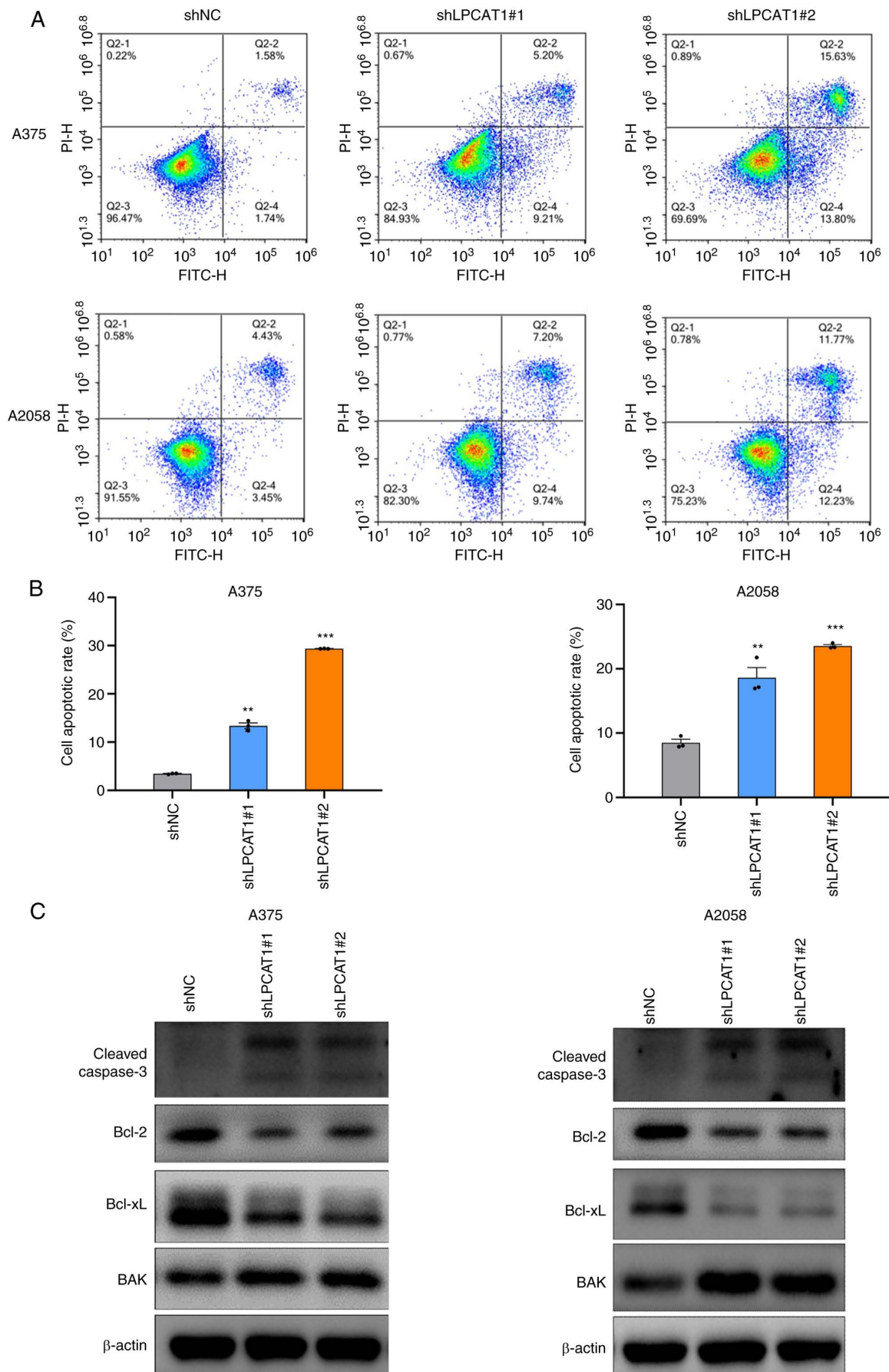


Figure 4. LPCAT1 knockdown promotes melanoma cell apoptosis. (A) Flow cytometric analysis of the apoptosis of A375 and A2058 cells transfected with control and LPCAT1 shRNA. (B) Quantification of cell apoptosis in (A). (C) Western blot analysis of cell apoptosis regulators in A375 and A2058 cells transfected with control and LPCAT1 shRNA. Data represent the mean \pm SEM of triplicates. ** $P < 0.01$ and *** $P < 0.001$ vs. shNC. LPCAT1, lysophosphatidylcholine acyltransferase 1; shNC, short hairpin RNA targeting negative control; shLPCAT1, short hairpin RNA targeting LPCAT1.

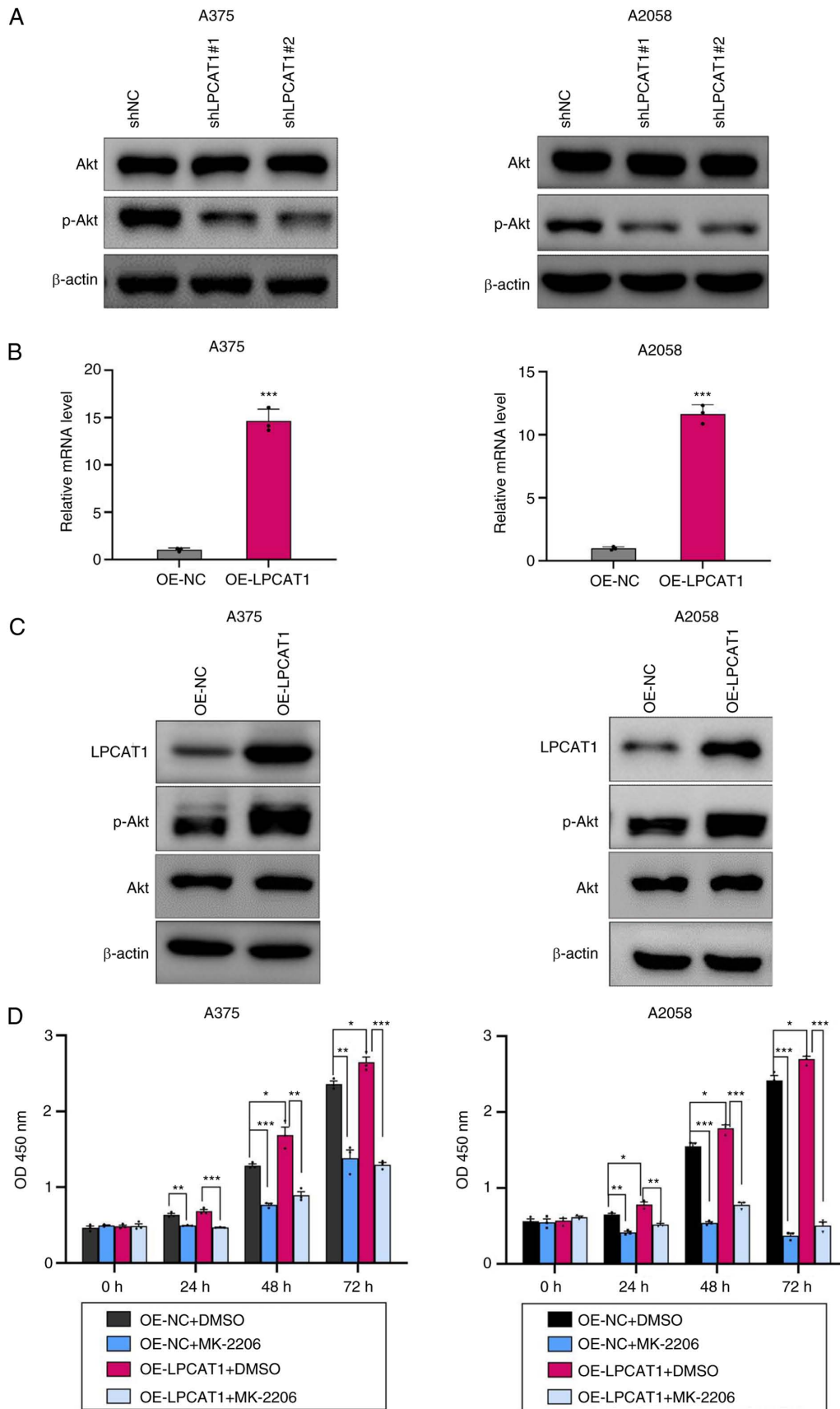


Figure 5. LPCAT1 facilitates melanoma cell growth via the Akt signaling pathway. (A) Western blot analysis of Akt signaling in A375 and A2058 cells transfected with control and LPCAT1 shRNA. (B) Relative mRNA level of LPCAT1 in A375 and A2058 cells transfected with control and LPCAT1 overexpression lentivirus. Data represent the mean \pm SEM of triplicates. *** P <0.001 vs. OE-NC. (C) Western blot analysis of LPCAT1 expression and Akt signaling in A375 and A2058 cells transfected with control and LPCAT1 overexpression lentivirus. (D) Cell viability of A375 and A2058 cells transfected with control and LPCAT1 overexpression lentivirus. Cells were treated with DMSO or 10 μ M MK-2206. Data represent the mean \pm SEM of triplicates. * P <0.05, ** P <0.01 and *** P <0.001 vs. respective control group. LPCAT1, lysophosphatidylcholine acyltransferase 1; shNC, short hairpin RNA targeting negative control; shLPCAT1, short hairpin RNA targeting LPCAT1; OE-NC, control overexpression lentivirus; OE-LPCAT1, LPCAT1 overexpression lentivirus.

metabolic reprogramming (31-33). Metabolic reprogramming contributes to the cell growth, aggressiveness and heterogeneity in melanoma. Accelerated lipid synthesis is among the most notable metabolic reprogramming features and can serve as an energy resource, membrane structural basis and carcinogenic signaling mediator (34). For instance, a previous study reported that phosphatidylcholine contents were increased and lysophosphatidylcholine contents were decreased in serum from mice with melanoma (35). The same study also demonstrated an elevated expression of LPCAT1 in B16F10 melanoma cancer cells and in tissue from mice with melanoma. The upregulation of LPCAT1 in tissue from mice with melanoma could be, at least partially, responsible for the metabolic profile change in mouse serum (35). In the present study, the expression of LPCAT1 in patient samples was detected and it was observed that LPCAT1 expression was increased in tissues from patients with melanoma, as compared with benign nevi. This result is consistent with previous findings on the melanoma-bearing mice and melanoma cell lines (35).

The present study aimed to explore the role of LPCAT1 in melanoma. LPCAT1 promoted melanoma cell proliferation by regulating the cell cycle and modulating cell death. LPCAT1 knockdown suppressed the G1/S cell cycle transition by decreasing the expression of cyclin D1. Additionally, this also facilitated melanoma cell apoptosis by upregulating the expression of cleaved caspase-3 and BAK, and downregulating the expression of Bcl-2 and Bcl-xL. A previous study by the authors demonstrated that LPCAT1 accelerated cutaneous squamous cell carcinoma cell growth by upregulating cyclin D1 expression (17). Furthermore, LPCAT1 inhibited cell apoptosis by decreasing the expression of cleaved caspase-3 and BAK, and increasing the expression of Bcl-xL without altering Bcl-2 expression in cutaneous squamous cell carcinoma (17). The differences in Bcl-2 expression between melanoma and cutaneous squamous cell carcinoma may be due to cancer types and context. However, the aforementioned findings suggest that the role of LPCAT1 has certain similarities in skin cancers, including the promotion of the proliferation, regulation of the cell cycle, and the modulation of the death of skin cancer cells.

The present study implicates LPCAT1 accelerated cell proliferation in an Akt-dependent manner in melanoma. Accumulating evidence has indicated that PI3K/Akt pathway is one of the most crucial signaling networks in melanoma (36). The activation of PI3K/Akt signaling regulates various essential cellular processes and the aberrant activation of Akt promotes melanoma pathogenesis. Akt is critical for the transformation from melanocytes to melanoma cells, thereby triggering the conversion of benign nevi to melanoma (37). Activated Akt signaling also culminates in an enhanced proliferation, decreased apoptosis and drug resistance in melanoma (38,39). p-Akt has been reported to serve as an independent prognostic marker, aiding towards clinical decisions (40). The results of the present study demonstrate that LPCAT1 may affect several pathophysiological functions of melanoma cells via Akt signaling. Moreover, relevant studies have detected the association between LPCAT, PI3K and Akt. Ding *et al* (41) demonstrated that the EGFR/PI3K/Akt cascade was the key downstream signaling pathway of LPCAT1 in lung adenocarcinoma. Furthermore, LPCAT1 promoted the

brain metastasis of lung adenocarcinoma via the upregulation of the PI3K/Akt/MYC pathway. Therefore, PI3K may be the key factor linking LPCAT1 and Akt in melanoma.

Progress made in therapeutics has changed the standard treatment strategies for melanoma. Targeted therapies and immunotherapies can be applied as the first-line treatment for advanced-stage or metastatic melanoma. Targeted therapies mainly involve the targeting of B-Raf proto-oncogene serine/threonine kinase (BRAF) and have a higher predictability of response (42,43). Immunotherapy is mainly based on immune checkpoint blockade and induces longer durable remissions (44-46). However, half of patients with melanoma treated with BRAF inhibitors develop resistance within the first 5 years of therapy (47). Melanoma cells have been reported to evade BRAF inhibitor therapies through the PI3K/Akt pathway (48,49). The dual inhibition of BRAF and the PI3K/Akt pathway has been shown to be effective against BRAF resistance in preclinical models (50). The resistance mechanisms of immunotherapies may also involve lipid signaling activities of melanoma cells, supporting the hypothesis of lipid signaling exploitation as a therapeutic target (51). Targeting Akt signaling and lipid metabolism may prevent or overcome resistance to BRAF inhibitors and immunotherapy. LPCAT1 can function as a node between Akt signaling and lipid metabolism against resistance. The currently available therapeutic interventions targeting LPCAT1 are still at the stage of basic research, without having been clinically applied. Regardless, He *et al* (20) hypothesized that several small molecule drugs may be administered as potential therapeutics for LPCAT1 by targeting at the differential expression genes that are co-expressed with LPCAT1, demonstrating the potential drugability of LPCAT1. These findings suggest that the therapeutic strategy targeting LPCAT1 may be promising for the treatment of melanoma.

In conclusion, the present study indicated the robust proliferative role of LPCAT1 in melanoma. Considering that targeting LPCAT1 inhibits cell proliferation via suppressing Akt signaling, therapeutics based on LPCAT1 may help advance targeted therapy and immunotherapy in melanoma.

Acknowledgements

The authors would like to thank Dr Yongping Shao and Dr Jiankang Liu for providing the experimental sites and technical assistance on cell culture.

Funding

The present study was supported by the National Natural Science Foundation of China (Grant nos. 81972938 and 82304015).

Availability of data and materials

The datasets used and/or analyzed during the current study are available from the corresponding author on reasonable request.

Authors' contributions

YuW, YH and YZ designed the experiments. YH, YuW and YaW conducted the experiments. YuW, YH, NW, RL, HT, WZ

and RB analyzed the data. YH and YuW wrote the manuscript. YZ and YH confirm the authenticity of all the raw data. All authors have read and approved the final manuscript.

Ethics approval and consent to participate

The use of patient tissues was approved by the Institutional Ethics Committee of the First Affiliated Hospital of Xi'an Jiaotong University (Xi'an, China; approval no. LLSBPJ-2023-222). Written informed consent was obtained from the patients prior to sample collection.

Patient consent for publication

Not applicable.

Competing interests

The authors declare that they have no competing interests.

References

- Miller AJ and Mihm MC Jr: Melanoma. *N Engl J Med* 355: 51-65, 2006.
- Lo JA and Fisher DE: The melanoma revolution: from UV carcinogenesis to a new era in therapeutics. *Science* 346: 945-949, 2014.
- Schadendorf D, van Akkooi ACJ, Berking C, Griewank KG, Gutzmer R, Hauschild A, Stang A, Roesch A and Ugurel S: Melanoma. *Lancet* 392: 971-984, 2018.
- Hughes MS, Zager J, Faries M, Alexander HR, Royal RE, Wood B, Choi J, McCluskey K, Whitman E, Agarwala S, *et al*: Results of a randomized controlled multicenter phase III trial of percutaneous hepatic perfusion compared with best available care for patients with melanoma liver metastases. *Ann Surg Oncol* 23: 1309-1319, 2016.
- Zhu Z, Liu W and Gotlieb V: The rapidly evolving therapies for advanced melanoma-towards immunotherapy, molecular targeted therapy, and beyond. *Crit Rev Oncol Hematol* 99: 91-99, 2016.
- Roberts P, Fishman GA, Joshi K and Jampol LM: Chorioretinal lesions in a case of melanoma-associated retinopathy treated with pembrolizumab. *JAMA Ophthalmol* 134: 1184-1188, 2016.
- Chapman PB, Jayaprakasam VS, Panageas KS, Callahan M, Postow MA, Shoushtari AN, Wolchok JD and Betof Warner A: Risks and benefits of reinduction ipilimumab/nivolumab in melanoma patients previously treated with ipilimumab/nivolumab. *J Immunother Cancer* 9: 2021.
- Nakanishi H, Shindou H, Hishikawa D, Harayama T, Ogasawara R, Suwabe A, Taguchi R and Shimizu T: Cloning and characterization of mouse lung-type acyl-CoA:lysophosphatidylcholine acyltransferase 1 (LPCAT1). Expression in alveolar type II cells and possible involvement in surfactant production. *J Biol Chem* 281: 20140-20147, 2006.
- Chen X, Hyatt BA, Mucenski ML, Mason RJ and Shannon JM: Identification and characterization of a lysophosphatidylcholine acyltransferase in alveolar type II cells. *Proc Natl Acad Sci USA* 103: 11724-11729, 2006.
- Kennedy EP and Weiss SB: The function of cytidine coenzymes in the biosynthesis of phospholipides. *J Biol Chem* 222: 193-214, 1956.
- Lands WE: Metabolism of glycerolipides; a comparison of lecithin and triglyceride synthesis. *J Biol Chem* 231: 883-888, 1958.
- Bridges JP, Ikegami M, Brilli LL, Chen X, Mason RJ and Shannon JM: LPCAT1 regulates surfactant phospholipid synthesis and is required for transitioning to air breathing in mice. *J Clin Invest* 120: 1736-1748, 2010.
- Moessinger C, Kuerschner L, Spandl J, Shevchenko A and Thiele C: Human lysophosphatidylcholine acyltransferases 1 and 2 are located in lipid droplets where they catalyze the formation of phosphatidylcholine. *J Biol Chem* 286: 21330-21339, 2011.
- Harayama T, Shindou H, Ogasawara R, Suwabe A and Shimizu T: Identification of a novel noninflammatory biosynthetic pathway of platelet-activating factor. *J Biol Chem* 283: 11097-11106, 2008.
- Cheng L, Han X and Shi Y: A regulatory role of LPCAT1 in the synthesis of inflammatory lipids, PAF and LPC, in the retina of diabetic mice. *Am J Physiol Endocrinol Metab* 297: E1276-E1282, 2009.
- Dai X, Han J, Qi Y, Zhang H, Xiang L, Lv J, Li J, Deng WT, Chang B, Hauswirth WW and Pang JJ: AAV-mediated lysophosphatidylcholine acyltransferase 1 (Lpcat1) gene replacement therapy rescues retinal degeneration in rd11 mice. *Invest Ophthalmol Vis Sci* 55: 1724-1734, 2014.
- Huang Y, Wang Y, Wang Y, Wang N, Duan Q, Wang S, Liu M, Bilal MA and Zheng Y: LPCAT1 promotes cutaneous squamous cell carcinoma via EGFR-mediated protein kinase B/p38MAPK signaling pathways. *J Invest Dermatol* 142: 303-313 e309, 2022.
- Wei C, Dong X, Lu H, Tong F, Chen L, Zhang R, Dong J, Hu Y, Wu G and Dong X: LPCAT1 promotes brain metastasis of lung adenocarcinoma by up-regulating PI3K/AKT/MYC pathway. *J Exp Clin Cancer Res* 38: 95, 2019.
- Bi J, Ichu TA, Zanca C, Yang H, Zhang W, Gu Y, Chowdhry S, Reed A, Ikegami S, Turner KM, *et al*: Oncogene amplification in growth factor signaling pathways renders cancers dependent on membrane lipid remodeling. *Cell Metab* 30: 525-538 e528, 2019.
- He RQ, Li JD, Du XF, Dang YW, Yang LJ, Huang ZG, Liu LM, Liao LF, Yang H and Chen G: LPCAT1 overexpression promotes the progression of hepatocellular carcinoma. *Cancer Cell Int* 21: 442, 2021.
- Ji W, Peng Z, Sun B, Chen L, Zhang Q, Guo M and Su C: LPCAT1 promotes malignant transformation of hepatocellular carcinoma cells by directly suppressing STAT1. *Front Oncol* 11: 678714, 2021.
- Du Y, Wang Q, Zhang X, Wang X, Qin C, Sheng Z, Yin H, Jiang C, Li J and Xu T: Lysophosphatidylcholine acyltransferase 1 upregulation and concomitant phospholipid alterations in clear cell renal cell carcinoma. *J Exp Clin Cancer Res* 36: 66, 2017.
- Shida-Sakazume T, Endo-Sakamoto Y, Unozawa M, Fukumoto C, Shimada K, Kasamatsu A, Ogawara K, Yokoe H, Shiiba M, Tanzawa H and Uzawa K: Lysophosphatidylcholine acyltransferase 1 overexpression promotes oral squamous cell carcinoma progression via enhanced biosynthesis of platelet-activating factor. *PLoS One* 10: e0120143, 2015.
- Liu Y, Yang C, Zhang Z and Jiang H: Gut microbiota dysbiosis accelerates prostate cancer progression through increased LPCAT1 expression and enhanced DNA repair pathways. *Front Oncol* 11: 679712, 2021.
- Han C, Yu G, Mao Y, Song S, Li L, Zhou L, Wang Z, Liu Y, Li M and Xu B: LPCAT1 enhances castration resistant prostate cancer progression via increased mRNA synthesis and PAF production. *PLoS One* 15: e0240801, 2020.
- Mansilla F, da Costa KA, Wang S, Kruhoffer M, Lewin TM, Orntoft TF, Coleman RA and Birkenkamp-Demtroder K: Lysophosphatidylcholine acyltransferase 1 (LPCAT1) overexpression in human colorectal cancer. *J Mol Med (Berl)* 87: 85-97, 2009.
- Lebok P, von Hassel A, Meiners J, Hube-Magg C, Simon R, Höflmayer D, Hinsch A, Dum D, Fraune C, Göbel C, *et al*: Up-regulation of lysophosphatidylcholine acyltransferase 1 (LPCAT1) is linked to poor prognosis in breast cancer. *Aging (Albany NY)* 11: 7796-7804, 2019.
- Zhao T, Zhang Y, Ma X, Wei L, Hou Y, Sun R and Jiang J: Elevated expression of LPCAT1 predicts a poor prognosis and is correlated with the tumour microenvironment in endometrial cancer. *Cancer Cell Int* 21: 269, 2021.
- Tao M, Luo J, Gu T, Yu X, Song Z, Jun Y, Gu H, Han K, Huang X, Yu W, *et al*: LPCAT1 reprogramming cholesterol metabolism promotes the progression of esophageal squamous cell carcinoma. *Cell Death Dis* 12: 845, 2021.
- Livak KJ and Schmittgen TD: Analysis of relative gene expression data using real-time quantitative PCR and the $2^{-\Delta\Delta CT}$ method. *Methods* 25: 1262, 2001.
- Ratnikov BI, Scott DA, Osterman AL, Smith JW and Ronai ZA: Metabolic rewiring in melanoma. *Oncogene* 36: 147-157, 2017.
- Gandhi SA and Kamm J: Skin cancer epidemiology, detection, and management. *Med Clin North Am* 99: 1323-1335, 2015.
- Ruocco MR, Avagliano A, Granato G, Vigliar E, Masone S, Montagnani S and Arcucci A: Metabolic flexibility in melanoma: A potential therapeutic target. *Semin Cancer Biol* 59: 187-207, 2019.

34. Pellerin L, Carrie L, Dufau C, Nieto L, Segui B, Levade T, Riond J and Andrieu-Abadie N: Lipid metabolic reprogramming: Role in melanoma progression and therapeutic perspectives. *Cancers (Basel)* 12: 3147, 2020.
35. Bao J, Liu F, Zhang C, Wang K, Jia X, Wang X, Chen M, Li P, Su H, Wang Y, *et al*: Anti-melanoma activity of forsythiae fructus aqueous extract in mice involves regulation of glycerophospholipid metabolisms by UPLC/Q-TOF MS-based metabolomics study. *Sci Rep* 6: 39415, 2016.
36. Davies MA: The role of the PI3K-AKT pathway in melanoma. *Cancer J* 18: 142-147, 2012.
37. Govindarajan B, Sligh JE, Vincent BJ, Li M, Canter JA, Nickoloff BJ, Rodenburg RJ, Smeitink JA, Oberley L, Zhang Y, *et al*: Overexpression of Akt converts radial growth melanoma to vertical growth melanoma. *J Clin Invest* 117: 719-729, 2007.
38. Cho JH, Robinson JP, Arave RA, Burnett WJ, Kircher DA, Chen G, Davies MA, Grossmann AH, VanBrocklin MW, McMahon M and Holmen SL: AKT1 activation promotes development of melanoma metastases. *Cell Rep* 13: 898-905, 2015.
39. Perna D, Karreth FA, Rust AG, Perez-Mancera PA, Rashid M, Iorio F, Alifrangis C, Arends MJ, Bosenberg MW, Bollag G, *et al*: BRAF inhibitor resistance mediated by the AKT pathway in an oncogenic BRAF mouse melanoma model. *Proc Natl Acad Sci USA* 112: E536-E545, 2015.
40. Dai DL, Martinka M and Li G: Prognostic significance of activated Akt expression in melanoma: A clinicopathologic study of 292 cases. *J Clin Oncol* 23: 1473-1482, 2005.
41. Ding JH, Ding XJ and Leng ZH: LPCAT1 promotes gefitinib resistance via upregulation of the EGFR/PI3K/AKT signaling pathway in lung adenocarcinoma. *J Cancer* 13: 1837-1847, 2022.
42. Dummer R, Flaherty KT, Robert C, Arance A, de Groot JWB, Garbe C, Gogas HJ, Gutzmer R, Krajsová I, Liskay G, *et al*: Encorafenib plus binimetinib versus vemurafenib or encorafenib in patients with BRAF-mutant melanoma (COLUMBUS): A multicentre, open-label, randomised phase 3 trial. *Lancet Oncol* 19: 603-615, 2018.
43. Long GV, Stroyakovskiy D, Gogas H, Levchenko E, de Braud F, Larkin J, Garbe C, Jouary T, Hauschild A, Grob JJ, *et al*: Dabrafenib and trametinib versus dabrafenib and placebo for Val600 BRAF-mutant melanoma: A multicentre, double-blind, phase 3 randomised controlled trial. *Lancet* 386: 444-451, 2015.
44. Hamid O, Robert C, Daud A, Hodi FS, Hwu WJ, Kefford R, Wolchok JD, Hersey P, Joseph R, Weber JS, *et al*: Five-year survival outcomes for patients with advanced melanoma treated with pembrolizumab in KEYNOTE-001. *Ann Oncol* 30: 582-588, 2019.
45. Schadendorf D, Hodi FS, Robert C, Weber JS, Margolin K, Hamid O, Patt D, Chen TT, Berman DM and Wolchok JD: Pooled analysis of long-term survival data from phase II and phase III trials of ipilimumab in unresectable or metastatic melanoma. *J Clin Oncol* 33: 1889-1894, 2015.
46. Brahmer JR, Tykodi SS, Chow LQ, Hwu WJ, Topalian SL, Hwu P, Drake CG, Camacho LH, Kauh J, Odunsi K, *et al*: Safety and activity of anti-PD-L1 antibody in patients with advanced cancer. *N Engl J Med* 366: 2455-2465, 2012.
47. Kozar I, Margue C, Rothengatter S, Haan C and Kreis S: Many ways to resistance: how melanoma cells evade targeted therapies. *Biochim Biophys Acta Rev Cancer* 1871: 313-322, 2019.
48. Van Allen EM, Wagle N, Sucker A, Treacy DJ, Johannessen CM, Goetz EM, Place CS, Taylor-Weiner A, Whittaker S, *et al*: The genetic landscape of clinical resistance to RAF inhibition in metastatic melanoma. *Cancer Discov* 4: 94-109, 2014.
49. Shi H, Hugo W, Kong X, Hong A, Koya RC, Moriceau G, Chodon T, Guo R, Johnson DB, Dahlman KB, *et al*: Acquired resistance and clonal evolution in melanoma during BRAF inhibitor therapy. *Cancer Discov* 4: 80-93, 2014.
50. Greger JG, Eastman SD, Zhang V, Bleam MR, Hughes AM, Smitheman KN, Dickerson SH, Laquerre SG, Liu L and Gilmer TM: Combinations of BRAF, MEK, and PI3K/mTOR inhibitors overcome acquired resistance to the BRAF inhibitor GSK2118436 dabrafenib, mediated by NRAS or MEK mutations. *Mol Cancer Ther* 11: 909-920, 2012.
51. Timar J, Hegedus B and Raso E: The role of lipid signaling in the progression of malignant melanoma. *Cancer Metastasis Rev* 37: 245-255, 2018.



Copyright © 2024 Wang et al. This work is licensed under a Creative Commons Attribution-NonCommercial-NoDerivatives 4.0 International (CC BY-NC-ND 4.0) License.